

HE Fang, ZHAO Zhengyu, NI Binbin, ZHANG Yuannong

Study on the ionospheric effects with different heat-conditions

© Higher Education Press and Springer-Verlag 2007

Abstract A numerical model has been developed. Based on the numerical simulation results, the spatial effects of the ionosphere, mainly consisting of the change on electron density (ED) and electron temperature (ET), heated by the high frequency (HF) pump wave have been analyzed quantitatively. Results are presented as the space-time evolution regulation on the main parameters of the ionosphere resulted by the HF heating waves under the different heat-conditions, just as different regions, such as high latitude and mid-low latitude; different heating power or frequency, such as under-dense heating and over-dense heating and regions at different altitudes. The heating effects in different regions with different heating conditions have been presented in figures. Finally, some primary conclusions are given by comparing the simulation results with experimental observation.

Keywords HF heating waves, ionospheric heating, heat-conditions

1 Introduction

Scientific experiments and theoretical researches indicate that a series of the local salient turbulences of the ionosphere will be aroused when the ground-based powerful HF waves are injected into it. Among all the turbulences, the evolution of the ED and ET is the most elementary effect. Actually, spatial effects in the ionosphere caused by the powerful HF waves are handled with very complicated plasma non-linear mechanism, and related to the effective radiation power (ERP) and the ionosphere background. With the enhancement of ERP, some nonlinear processes just as saturation and transition which are caused by the artificial ionospheric modification occur in different layers. The higher level effects exist steadily only when ERP reaches the relative threshold.

Translated from *Chinese Journal of Radio Science*, 2006, 21(4): 525–531 [译自: 电波科学学报]

HE Fang (✉), ZHAO Zhengyu, NI Binbin, ZHANG Yuannong
School of Electronic Information, Wuhan University, Wuhan 430079, China
E-mail: Ares123628@yahoo.com.cn

The interaction between the powerful HF waves and the ionospheric plasma is a nonlinear physical process. It is related to the chemical reactions of ionospheric ions, the wave-particle reactions, the transition and absorption of electromagnetic waves power and the geomagnetic field makes it more complicated. The ionosphere shows the different characteristics in different layers, so do the heating effects caused by the powerful HF waves. Generally speaking, the foundation of artificial ionospheric modification by ground-based powerful HF waves is the nonlinear characteristic brought from the interactions between the near-earth space and strong electric field. Its dielectric constant and electric conductivity are related to the electric field strength, whereas the electric current is no longer proportional to the electric field strength. Various instabilities may occur and the superposition principle is unavailable. There are two sorts of nonlinear effects [1–10]: one is the Ohm heating in ionosphere, as a kind of typical nonlinear process; the other is the parametric instability caused by the interactions between nonlinear waves. When the feature scale of the disturbed plasma region is much greater than the electronic mean free path, especially in the lower ionosphere, the Ohm heating is the dominant effect. However, in the unstable state process, the parametric instability takes its main position especially in the higher ionosphere.

The Ohm heating theory and numerical analysis model of ionosphere modification by high frequency wave have been developed by Banks [11], Bernhardt [12] and Schunk [13]. In this paper, the temporal-spatial evolutions of ionospheric parameters and heating effects were discussed on the basis of the available works. The simulation results are also contrasted with the experimental ones operated by EISCAT at the same latitude.

2 Models and heating parameters

2.1 Heating model and ionosphere model

The method to establish the ionosphere model heated by HF wave has been given by Ni [14] and Huang [15].

The dynamic function can be expressed in the form

$$n_e v_e = -D \left\{ \frac{\partial}{\partial S} [n_e k_B (T_e + T_i)] + \sum_x m_x n_x \bar{g} \cdot \bar{B} / B \right\} \quad (1)$$

The continuously equation can be expressed in the form

$$\frac{\partial n_x}{\partial t} + \frac{\partial}{\partial z} n_x u_x = S_x(z) + P_x(z, t) - \beta_x(z, t) \quad (2)$$

The electron energy conservation equation can be expressed in the form

$$\begin{aligned} & \frac{3}{2} k_B (n_e \frac{\partial T_e}{\partial t} + n_e u_e \frac{\partial T_e}{\partial z}) + k_B n_e T_e \frac{\partial u_e}{\partial z} \\ & = \frac{1}{\sin \theta} \frac{\partial}{\partial z} \left(\frac{\kappa_e}{\sin \theta} \frac{\partial T_e}{\partial z} \right) + Q_{HF}(z, t) + Q_0(z) - L_e(z, t) \end{aligned} \quad (3)$$

The parameter variation has been considered only in the z direction in Eqs. (1)–(3).

The geomagnetic model can be written as

$$B_A = B_0 \left(\frac{637 \text{ 1.2}}{637 \text{ 1.2} + h} \right)^3 \sqrt{1 + 3 \sin^2 \theta} \quad (4)$$

where h is the altitude, and B_0 is the ground magnetic field strength.

Background ionosphere model in the simulation is given by international reference ionosphere model (IRI-95), and the ionosphere is taken to be considered as homosphere. At this rate, the ionospheric parameter is only changeable with altitude.

To take typical latitude into consideration, three regions are chosen as follows: Alaska (145.1°W, 62.39°N) for high latitude, Wuhan (114.35°E, 30.5°N) and Fuzhou (119.3°E, 26.0°N) for middle-low latitude. For the European incoherent scatter (EISCAT) and Arecibo system are at the same latitude, it is likely to compare the simulation results with the experimental observation to validate the accuracy of simulation research.

Because different kinds of ions and neutral molecules dominate the main heating effects at different altitudes, the four neutral molecules: N_2 , O_2 , O and He , and three ions: O_2^+ , NO^+ and O^+ , in D and E layers are taken into consideration and the neutral molecules effects in F layer are ignored because of their weak interaction with electrons.

2.2 Heating parameters

The heating parameters are taken as below.

- 1) Heating hours: 1 200 local time (LT), 0 000 LT.
- 2) ERP: 10, 20, 50, 100, 200, 300, 400, 500, 1 000 MW.
- 3) Transmitter frequency: 2, 3, 4, 5, 6, 7, 8, 9, 10, 11, 12, 13, 14 MHz.
- 4) Initial electron density: obtained from IRI-95 model.
- 5) Initial electron temperature: obtained from IRI-95 model.
- 6) Simulation altitudes: 60–400 km.

3 Analysis of temporal-spatial evolution of ionospheric parameters

Based on the heating parameters selected above, the numerical simulation has been made in the six different ionosphere backgrounds. The trend of ED and ET evolution has been presented in Figs. 1–12.

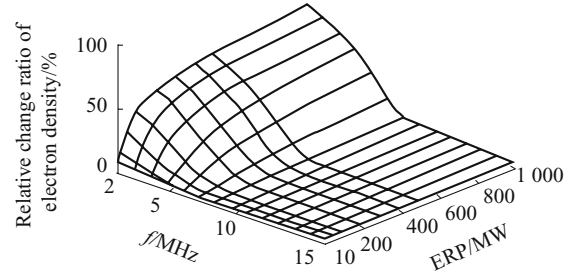


Fig. 1 Relative change ratio of ED in Alaska at 1200 LT

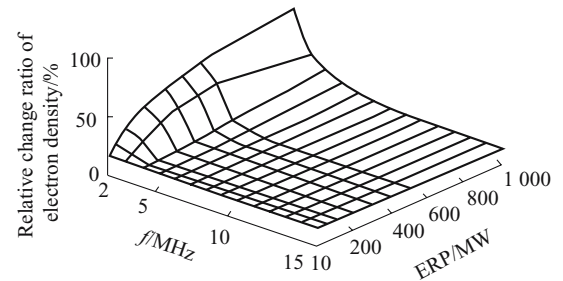


Fig. 2 Relative change ratio of ED in Alaska at 0000 LT

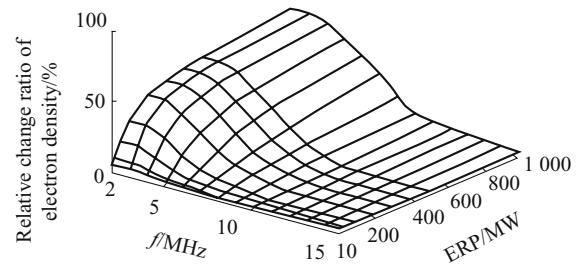


Fig. 3 Relative change ratio of ED in Wuhan at 1200 LT

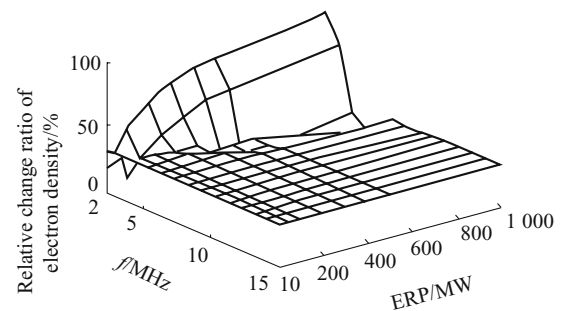


Fig. 4 Relative change ratio of ED in Wuhan at 0000 LT

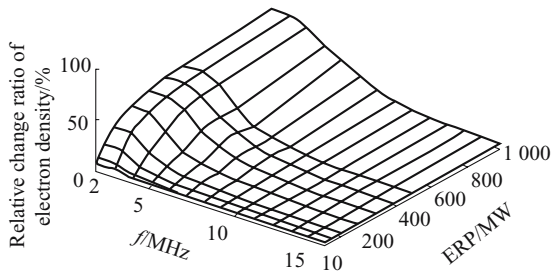


Fig. 5 Relative change ratio of ED in Fuzhou at 1200 LT

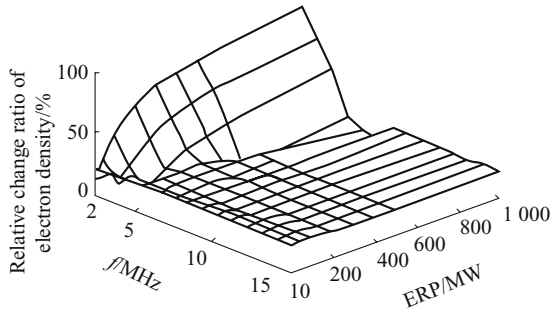


Fig. 6 Relative change ratio of ED in Fuzhou at 0000 LT

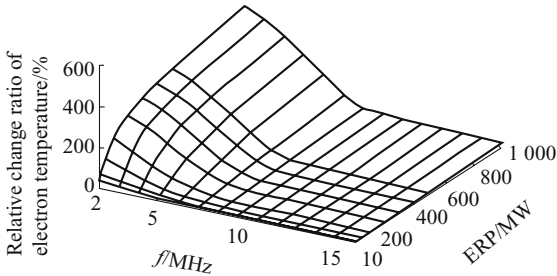


Fig. 7 Relative change ratio of ET in Alaska at 1200 LT

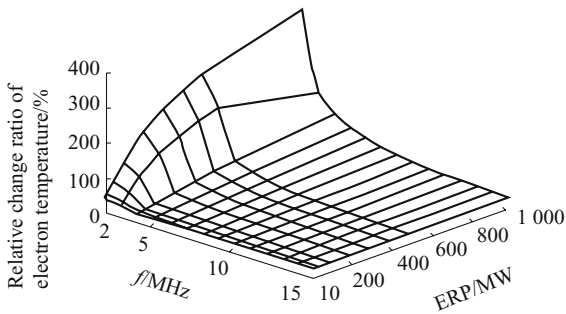


Fig. 8 Relative change ratio of ET in Alaska at 0000 LT

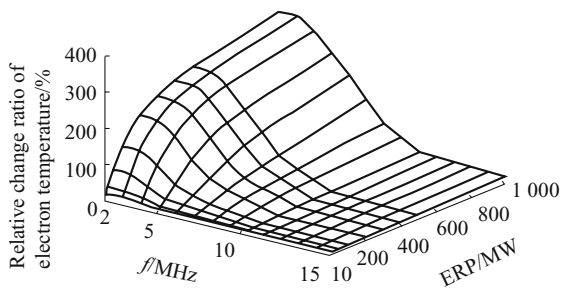


Fig. 9 Relative change ratio of ET in Wuhan at 1200 LT

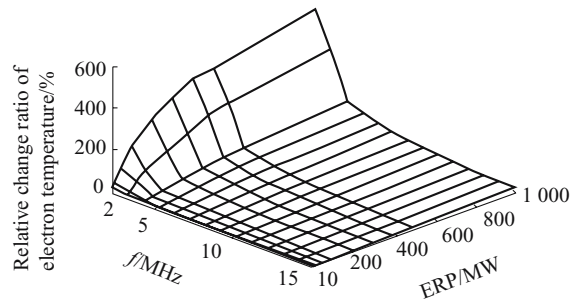


Fig. 10 Relative change ratio of ET in Wuhan at 0000 LT

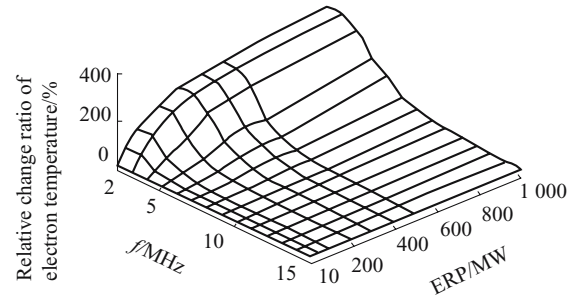


Fig. 11 Relative change ratio of ET in Fuzhou at 1200 LT

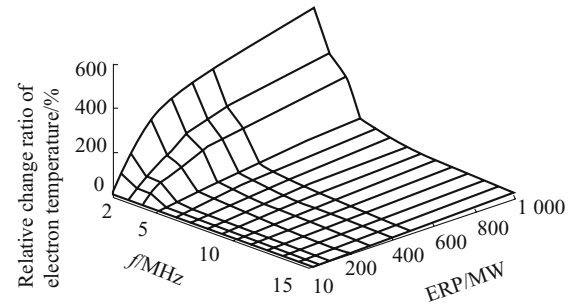


Fig. 12 Relative change ratio of ET in Fuzhou at 0000 LT

In order to focus on the maximum evolution state of ionospheric parameters which are paid attention, the heating duration is set to 500 s on the basis of the ionospheric electron saturation time. As a result, the ionospheric electron state can be surely saturated.

Figures 1–6 show the relative change of ED in six various ionosphere backgrounds with different transmitter frequency and various ERP. Figures 7–12 show the relative change of ET in the corresponding backgrounds respectively. Some primary conclusions can be gained from the figures.

1) The value of transmitter frequency and ERP are the two significant variables on which the heating effects mainly depend. Whether the heating condition is under under-dense model or over-dense model depends on the transmitter frequency and the latter variable denotes the heating intensity. When in the over-dense model, the remarkable evolution of ED occurs at the reflection altitude. With the increase in the transmitter frequency, the heating effects are weakened. Whereas, in the under-dense model, the heating effects depend on both particle collision process and transport

process. Moreover, with the increase in the wave frequency, there is the same trend of ED evolution as in the over-dense model, but it is less affected from the value of frequency. On the other hand, with the increase in ERP, the ionosphere evolution in the over-dense model changes much faster than that in the under-dense model, for the ionosphere absorption loss has the opposite trend against the transmitter frequency. In the higher band, the ionosphere absorption loss decays, that is to say, the wave energy which is conveyed to the ionosphere decreases. As a result, the change of ED and ET becomes less. In the meanwhile, the simulation results indicate that the heating effects and transmitter frequency have no inverse proportion relationship. However, the effects have no direct proportion relationship with ERP either.

2) In the process of heating, the evolution of ET is the most significant effect with an obvious increase; whereas the evolution of ED is not so remarkable, even in the over-dense model, it may decrease in some cases. The fluctuation of ED and ET is caused by its recombination and diffusion.

3) The heating effects obtained at 0 000 LT are more significant than those obtained at 1 200 LT. In the same heating condition, the heating evolution at night is more effective. The reason is that the initial parameters of ionosphere at night are lower than those in daytime.

4) With the same heating parameters, the heating effects in Alaska are more significant than the effects in Wuhan and Fuzhou. In addition, the effects in Wuhan are more obvious than those in Fuzhou in some sort. It is indicated that the heating effects at high latitude are more remarkable than that in mid-low latitude regions. In some specific conditions, salient turbulence in high latitude regions can be observed, but not in the same way in mid-low regions. However, by increasing the ERP some remarkable evolution turns out even in mid-low regions.

4 Analytical comparison of experimental results

Combining the simulation work to carry out the contrast analysis, the EISCAT experimental results (Robinson, 1989; Stocker, 1992) have been selected in order to validate the accuracy of the simulation results and the possibility of ionosphere heating experiment in the mid-low latitude regions.

Because the result from the Alaska heating experiment is unavailable, the comparison is only taken between the EISCAT experiment results and the simulation results.

Figure 13 shows the increase in ET with 4.5 MHz, 100 MW heater signal versus time; Fig. 14 shows the increase in ED with 4.544 MHz, 240 MW heater signal at the reflection altitude versus time. The evolution shown in the two figures is observed by EISCAT radar.

1) Comparison of electron temperature with the same ERP

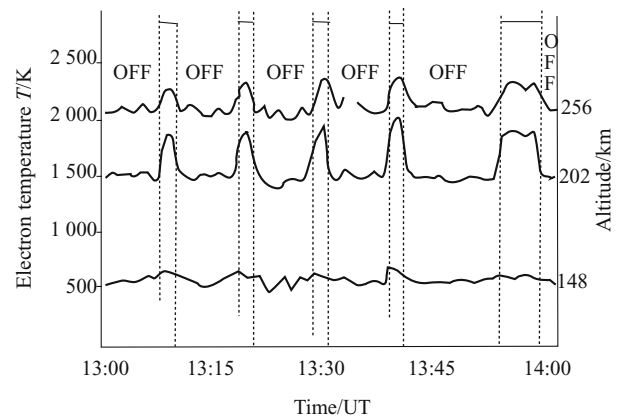


Fig. 13 Increase in electron temperature observed by EISCAT radar

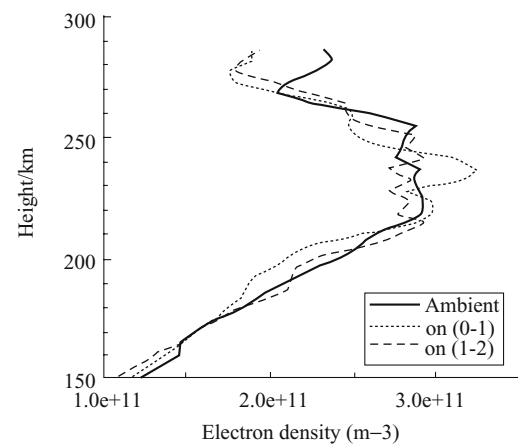


Fig. 14 Increase in electron density observed by EISCAT radar

Heated with 100 MW, 4.5 MHz signal, the relative change ratio of ET at an altitude of 202 km is approximately 20% in EISCAT radar observation. And the simulation results indicate that heated with 100 MW, 6 MHz signal in Alaska, the relative change ratio of electron temperature at an altitude of 210 km is approximately 25% at daytime. Although there inevitably exist some experimental errors, in general, the practical and theoretical results agreed well. However, heated in Fuzhou with the same heating parameters, the relative change ratio of ET at an altitude of 202 km is about 18% because of the more effective heating efficiency in high latitude regions.

2) Comparison of electron density with same heater ERP

Heated with 240 MW, 4.544 MHz signal, the relative change ratio of ED at an altitude of 210 km is approximately 8% in EISCAT radar observation. In Fig. 5 the simulation results indicate that heated with 240 MW, 6 MHz signal in Alaska, the relative change ratio of electron density at an altitude of 210 km is approximately 10% at daytime. However, heated in Fuzhou with the same heating parameters, the relative change ratio of ED at an altitude of 202 km is about 7% because of the more effective heating efficiency in high latitude regions.

3) Comparison of electron temperature with the same heater frequency

Heated with 100 MW, 4.5 MHz signal, the relative change ratio of ET at an altitude of 256 km is approximately 15% in EISCAT radar observation. The simulation results indicate that heated with the same heater parameters in Alaska, the relative change ratio of ET at an altitude of 250 km is approximately 20% at daytime. However, heated in Fuzhou and Wuhan with the same heating parameters, the relative change ratio of ET is both about 8% because of the more effective heating efficiency in high latitude regions.

4) Comparison of electron density with the same heater frequency

Heated with 240 MW, 4.544 MHz signal, the relative change ratio of ED at an altitude of 250 km is approximately 5% in EISCAT radar observation. The simulation results indicate that heated with 400 MW, 4.544 MHz signal in Alaska and Fuzhou, the relative change ratio of ED is approximately 2% and 1% respectively at daytime due to the more effective heating efficiency in high latitude regions.

5 Conclusions

Comparing simulation results with the experimental observation, there appeared a similar heating phenomenon in the mid-low latitude as well as in high latitude. It is feasible to carry out the ground-base HF heating experiment in mid-low latitude regions, though the heating effects are weaker. The reasons of feasibility are presented as follows.

1) By comparing the EISCAT experiment with the simulation results of Alaska, Fuzhou and Wuhan, the evolution conformance can be confirmed. The comparison of ED and ET has been made while some introduced errors can be neglected.

2) From the limited experiment results in Arecibo, significant electron evolution has been observed. It is indicated that the practicability of the mid-low latitude experiments in China and the feasibility of the experiment with the proper heater parameters in Fuzhou and Wuhan are available.

Acknowledgements This work was supported by the Hi-Tech Research and Development Program of China (No. 2004733AA101).

References

1. DuBios D F, Goldman M V. Radiation-induced instability of electron plasma oscillations. *Phys Rev Lett*, 1965, 14(14): 544–546
2. DuBios D F, Goldman M V. Parametrically excited plasma fluctuations. *Phys Rev*, 1967, 164(1): 207–222
3. Silin V P. Interaction of a strong high frequency electromagnetic field with plasma. In: *Proc of the Eighth Int Conf Phenom Ionized Gases*, 1968b, 205–237
4. Silin V P. Anomalous nonlinear dissipation of high frequency radio waves in plasma. *Soviet Physics*, 1973a, 15(3): 742–758
5. Nishikawa K. Parametric excitation of coupled waves I. General formulation. *Journal of the Physical Society of Japan*, 1968a, 24(4): 916–922
6. Nishikawa K. Parametric excitation of coupled waves II. Parametric plasmon photon interaction. *Journal of the Physical Society of Japan*, 1968b, 24(5): 1 152–1 158
7. Gurevich A V. Radio wave effect on the ionosphere in the F2 layer region. *Geomagn Aeron*, 1967, 7(1): 291–297
8. Gurevich A V. *Nonlinear Phenomena in the Ionosphere*. New York: Springer-Verlag, 1978
9. Fejer J A. Ionospheric modification and parametric instabilities. *Reviews of Geophysics and Space Physics*, 1979, 17(1): 135–153
10. Perkins F W. Parametric instabilities and ionospheric modification. *Journal of Geophysics Research*, 1974, 79(4): 1 478–1 496
11. Banks P M, Kocharts G. *Aeronomy: Parts A and B*. New York: Academic Press, 1973
12. Bernhardt P A, Duncan L M. The feedback-diffraction theory of ionospheric heating. *Atmos Terr Phys*, 1982, 44(12): 1 061–1 074
13. Schunk R W, Walker J C. Theoretical ion densities in the lower ionosphere. *Space Physics*, 1980, 18: 813
14. Ni Binbin, Zhao Zhengyu, Xiang Wei, et al. Numerical modeling of ionospheric modification with powerful HF pump waves. *Chinese Journal of Radio Science*, 2004, 19(3): 274–279 (in Chinese)
15. Huang Wengeng, Gu Shifen. Ionospheric heating by powerful high-frequency. *Chinese Journal of Radio Science*, 2004, 19(3): 296–300 (in Chinese)